Probing the Sub-Structures of Solar Flare Ribbons

Vishal Singh [1] Eamon Scullion [1] Gert Botha [1]
Natasha Jeffrey [1] Malcolm Druett [2]

[1]Northumbria University, Newcastle Upon Tyne, England [2]KU Leuven, Belgium.

Ribbons and riblets

The primary mechanism driving solar flares is magnetic reconnection, which facilitates the transfer of energy from the magnetic field to the plasma, resulting in the acceleration of particle beams composed of electrons and ions. In addition to the energy deposited locally in the coronal plasma, energy is also transferred to the chromosphere through the impact of these electron beams, leading to the emission of Hydrogen at 656.28 nm (Hα) and the formation of elongated bright "ribbons" [2].

Recent high-resolution observations from the Swedish 1-m Solar Telescope (SST) CRISP, with a spatial scale of 43 km per pixel and a temporal cadence of 0.2s, have provided an unprecedented opportunity to examine these ribbons and their substructures, referred to as "riblets". In this study, we present a comprehensive statistical analysis of the substructures of flare ribbons for an X-class solar flare observed on 10 June 2014.

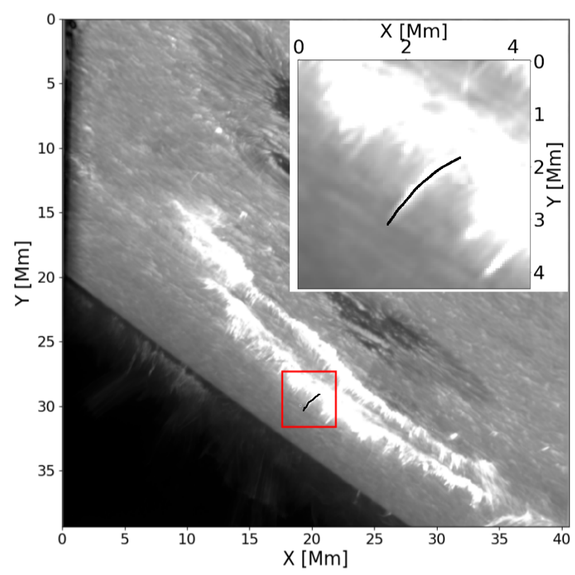

(a) A snapshot with one riblet track

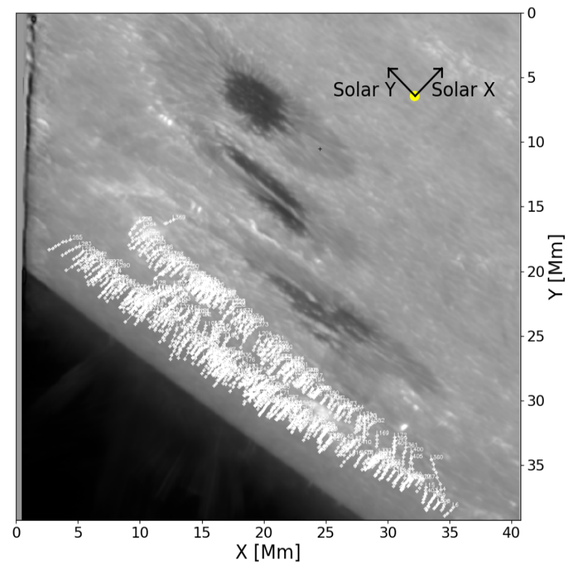

(b) All the tracked riblets (white dotted lines)

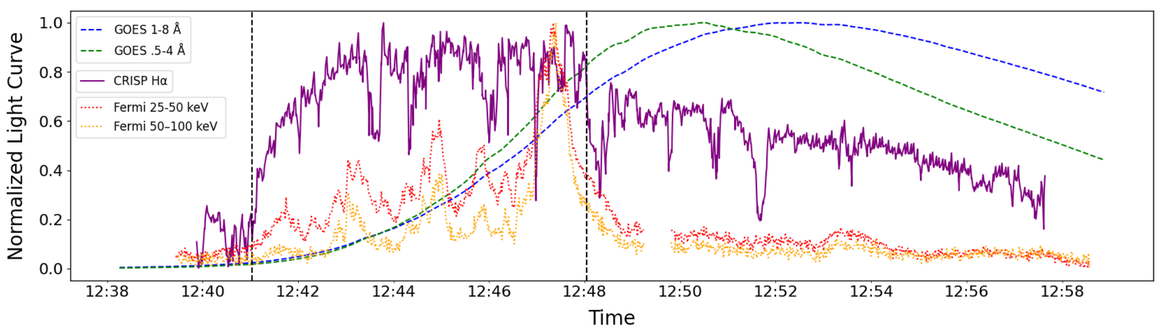

(c) Comparative light curves (GOES, CRSIP and Fermi) for our flare

The ribbons observed at the flare X-ray peak are presented in Fig 1a, with the semi-automated detection of riblets within the ribbons presented in Fig 1b. The evolution of riblet formations are compared against the evolution of the brightening of the ribbons in the EUV channels and corona from SDO/AIA in Fig 1c. There appears to be a correspondance between the start of the riblet formations (first vertical black dashed line) and the start of the hard X-ray emission as observed by FERMI and with GOES Soft X-rays peaking after the riblet formation peak time (second vertical black dashed line). Indicative of multiple electron-ion Bremsstrahlung emission as a mechanism for the formation of the riblets.

Riblet Evolution

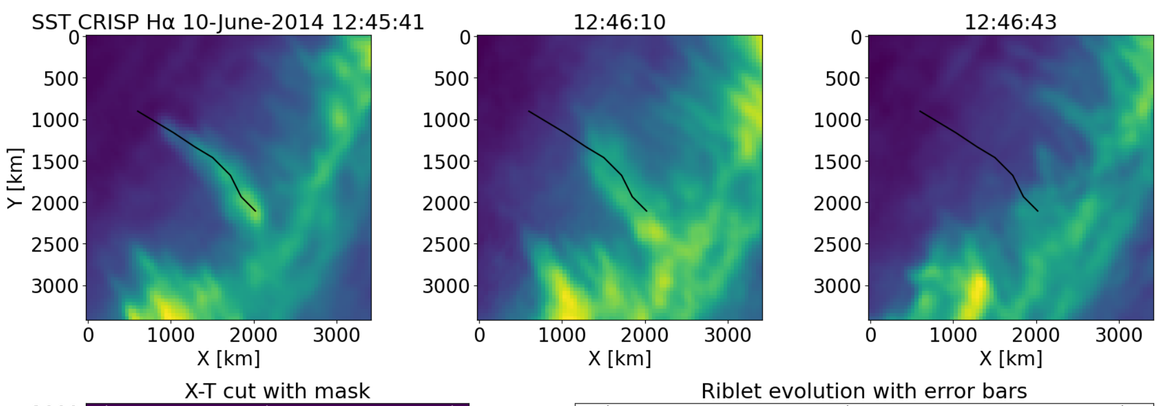

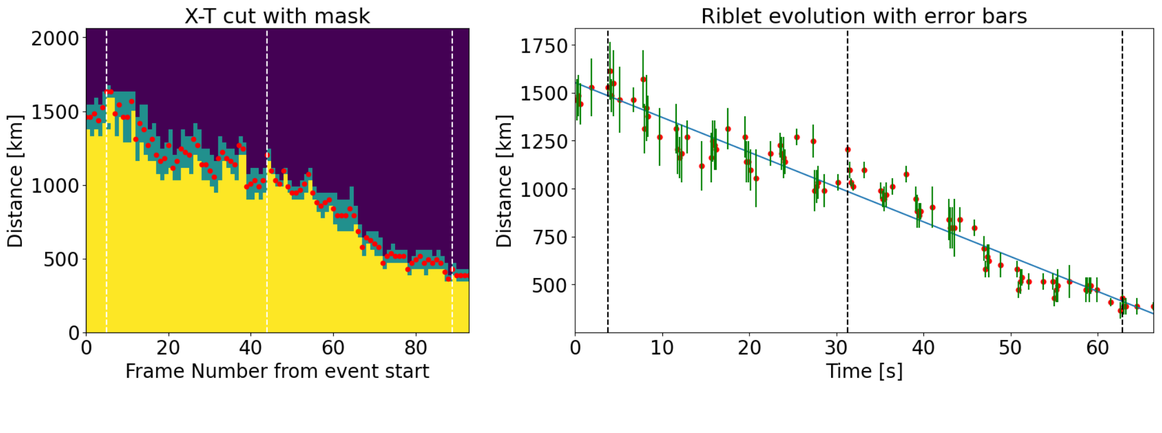

Figure 2. Riblet evolution of a typical constant velocity riblet. **Row 1:** Frames with the tracked riblet (black line) at different times in the life of the riblet. **Row 2 (a):** Evolution of intensities of the tracked pixels (riblet) over time. The red dots represent the tip of the riblet, as determined by masking. The green section indicates the region of uncertainty between the riblets and the background during our observation ($\mu \pm \sigma$). The yellow represents the signal ($> \mu + \sigma$), while the violet represents the background ($< \mu - \sigma$). The vertical dashed white lines point out the time of the frames in (a). **Row 2 (b):** The evolution of the length of the riblet with time. Tip of the riblet (red dots), uncertainty in the length (green bars) and a first-order polynomial fit (blue line). The vertical black dotted lines point out the time of the frames in Row 1.

To create the mask in Fig 2, we followed these steps: First, we selected a frame with minimal activity and another with ribbons, then plotted their respective intensity histograms. We calculated the difference between these histograms, isolating the peak corresponding to riblet activity. The intensity value with the maximum count from this peak was identified. This procedure was repeated for all frames with good seeing quality and ribbon activity, using the same quiet frame for comparison. Finally, the histogram of the calculated intensity values was fitted with a Gaussian profile.

Kinematic Statistics

We present the statistical analyses of the 230 tracked riblets, illustrated in Fig 3. For the nonlinear cases, the average speed is utilized for comparison with the linear cases.

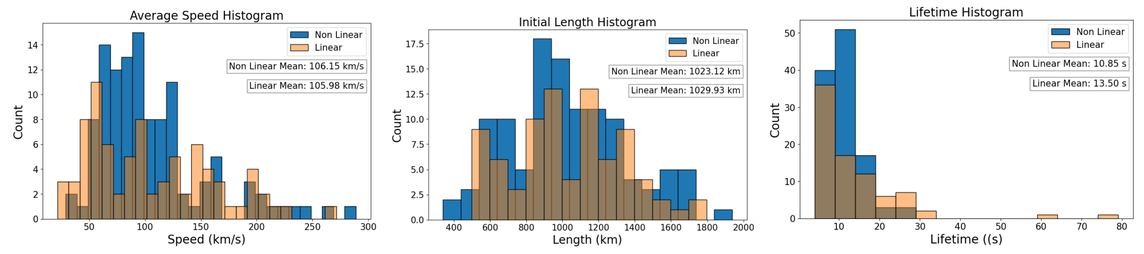

Figure 3. Average Speed, Initial Length and Lifetimes of the tracked riblets split into linear and non linear populations.

Projection effects

If we assume all riblets are linear and the non linear profiles are in fact coming from curvature of riblets towards or away from the line of sight, and account for that, the updated statistics are as follows,

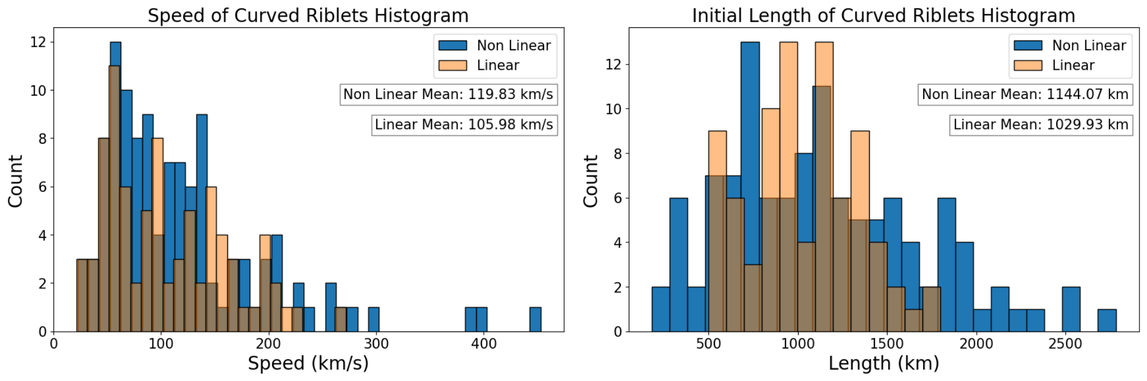

Spatial Energy Population Distribution

We examine the population distribution of linear and nonlinear riblets across different contour levels for AIA 304 Å, AIA 1700 Å, and RHESSI 25-50 keV. Our analysis reveals that the majority of riblets are concentrated within the lower energy contour levels, with no significant difference observed in the distribution between linear and nonlinear cases as seen in Fig 5.

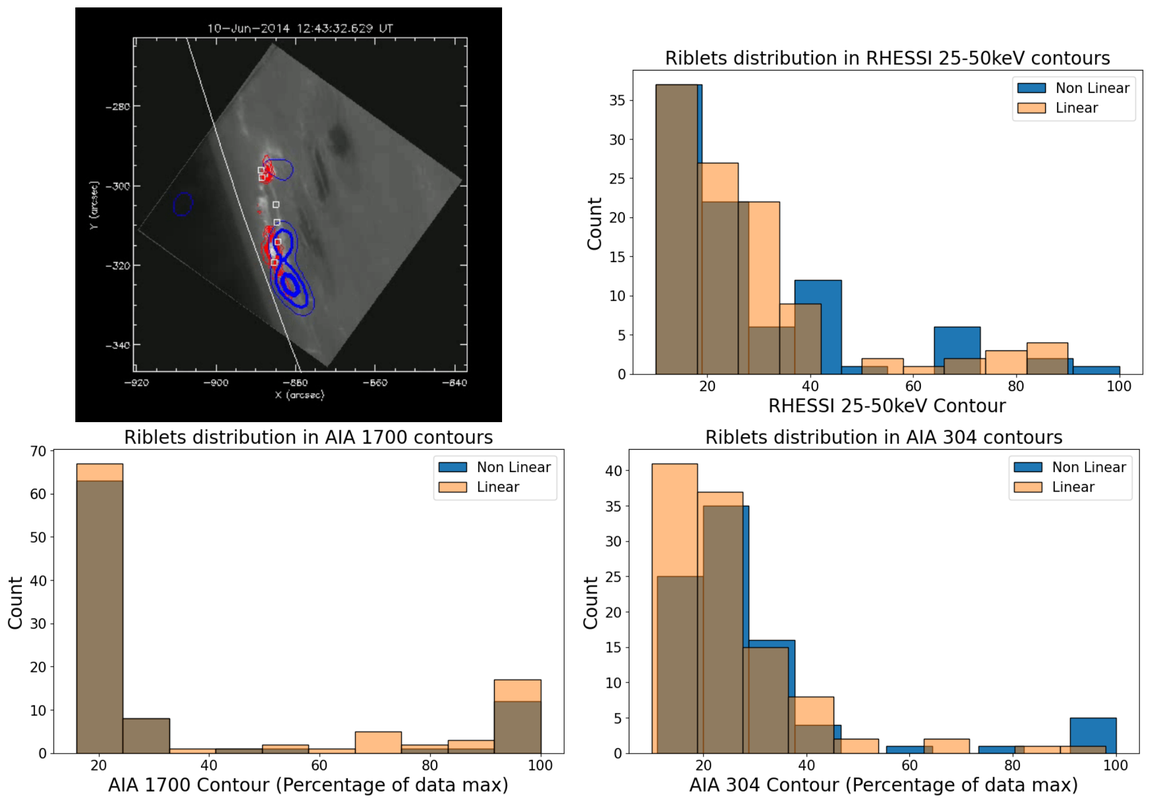

Figure 5. (a) CRISP observation with AIA 304 Å (red) and RHESSI 25-50 keV contours (blue). The white squares represent riblet positions at the time of the snapshot. (b)-(c)-(d) Population distribution of riblets in RHESSI, AIA 1700 and AIA 304 contours respectively

Conclusions and What's next

- Our study indicates that riblets are highly dynamic and transient phenomena, characterized by an average lifetime of 11.99 seconds and an average velocity of 106.1 km/s.
- By applying the masking technique, we were able to extract more refined velocity profiles, which allowed for a deeper analysis of the distribution of riblet velocities and accelerations.
- No significant differences were observed between the linear and non-linear cases in terms of their key parameters, including lifetime, length, speed, or their spatial and temporal distributions.
- Further investigations are necessary across flares of different classes to achieve statistically significant results.
- Future work should include attempts to replicate the linear and non-linear profiles through numerical simulations using models such as RADYN and HYDRO2GEN.

References

[1] M. Druett, Eamon Scullion, Valentina Zharkova, Sarah Matthews, Sergei Zharkov, and Luc Rouppe Van der Voort. Beam electrons as a source of Hα flare ribbons. *Nature Communications*, 8(1):15905, August 2017.

[2] L. Fletcher, B. R. Dennis, H. S. Hudson, S. Krucker, K. Phillips, A. Veronig, M. Battaglia, L. Bone, A. Caspi, Q. Chen, P. Gallagher, P. T. Grigis, H. Ji, W. Liu, R. O. Milligan, and M. Temmer. An observational overview of solar flares. *Space Science Reviews*, 159(1-4):19–106, September 2011.

[3] G. B. Scharmer, G. Narayan, T. Hillberg, J. de la Cruz Rodriguez, M. G. Löfdahl, D. Kiselman, P. Sütterlin, M. van Noort, and A. Lagg. CRISP Spectropolarimetric Imaging of Penumbral Fine Structure. *The Astrophysical Journal*, 689(1):L69–L72, December 2008.